PERGAMON

International Journal of Heat and Mass Transfer 45 (2002) 2815–2821

International Journal of HEAT and MASS TRANSFER

www.elsevier.com/locate/ijhmt

Technical Note

A new numerical method to simulate the non-Fourier heat conduction in a single-phase medium

Qing-Mei Fan, Wen-Qiang Lu *

Division of Thermal Science, Department of Physics, The Graduate School of the Chinese Academy of Sciences, P.O. Box 3908, Beijing 100039, China

Received 2 March 2001; received in revised form 8 November 2001

Abstract

Many non-equilibrium heat conduction processes can be described by the macroscopic dual-phase lag model (DPL model). In this paper, a numerical method, which combines the dual reciprocity boundary element method (DRBEM) with Laplace transforms, is constructed to solve such mathematical equation. It is used to simulate the non-Fourier phenomenon of heat conduction in a single-phase medium, then numerically predict the differences between the thermal diffusion, the thermal wave and the non-Fourier heat conduction under different boundary conditions including pulse for one- and two-dimensional problems. In order to check this numerical method's reliability, the numerical solutions are still compared with two known analytical solutions.

Keywords: Non-Fourier heat conduction; DPL model; Laplace transform; DRBEM; Thermal wave model

1. Introduction

In practical engineering problems, since heat sources such as lasers and microwaves with extremely short durations, very high frequencies or quite high heat-flux densities, are widely used, non-Fourier heat-conduction phenomenon has been found in many mediums [1–3]. Many heat transfer researchers have attached much importance to the potentially practical values of the non-Fourier heat conduction in many applications, such as rapid metal thawing and solidifying process, surface thermal processing by laser, temperature control of superconductor, laser and freezing surgery, rapid drying, etc. Therefore, the non-Fourier heat conduction has become one of hotspots in the field of heat transfer.

There are many physical models of non-Fourier heat conduction [4]. For the single-phase medium, these models can be separated into the microscopic two-step model [5,6] and the macroscopic dual-phase lag model [7]. The former considers that when the characteristic time of thermal process is comparable with the phonon–electron thermal relaxation time, the phonon–electron interaction dominates the short time heat-transfer process. The latter considers the lag of two macroscopic phases: temperature gradient and heat flux. Although the latter does not consider the microscopic reasons of the heat-transfer process on macroscopic level, many works have found that the two models can be expressed by the mathematical equation with the same mathematical characters under certain conditions [4,7–9]. Therefore, it is important to analyze the mathematical equation and its solution method.

The basic formulation of the dual-phase lag model (DPL model) in a single-phase medium is given by Tzou's formula [7]:

$$\vec{q} + \tau_q \frac{\partial \vec{q}}{\partial t} = -k\nabla T - k\tau_t \frac{\partial}{\partial t}\nabla T, \tag{1}$$

where $\vec{q}$ is the heat flux, T is the temperature and k is the thermal conductivity. τ_q and τ_t are the delay times in establishing heat flux and temperature gradient, respectively. The energy conservation equation without convection and radiation can be written as follows:

* Corresponding author. Tel.: +86-10-6239-5850; fax: +86-10-6821-5010.

E-mail address: luwq@sun.ihep.ac.cn (W.-Q. Lu).

0017-9310/02/$ - see front matter
PII: S0017-9310(01)00364-7

Nomenclature

c	specific heat	α	thermal diffusivity
k	thermal conductivity	β	dimensionless time, $t/(l^2/\alpha)$
l	length in the x-direction	η	dimensionless length in the y-direction, y/l
n	unit outward normal to the boundary Γ	θ	dimensionless temperature, $(T-T_0)/(T_w-T_0)$
q	temperature gradient, $\partial\theta/\partial n$		
$\bar{q}$	Laplace transformation of q, $\partial\bar{\theta}/\partial n$	$\bar{\theta}$	Laplace transformation of θ
$\bar{q}^*$	$\bar{q}^* = \partial\bar{\theta}^*/\partial n$	$\bar{\theta}^*$	fundamental solution, $(1/2\pi)\ln(1/r)$
$\hat{\bar{q}}$	$\hat{\bar{q}} = \partial\hat{\bar{\theta}}/\partial n$	$\hat{\bar{\theta}}$	particular solution, $(r^2/4)+(r^3/9)$
$\vec{q}$	heat flux	λ	Laplace transform parameter
t	time	ξ	dimensionless length in the x-direction, x/l
T	temperature	ρ	density
T_0	initial temperature	τ_q	delay time in establishing heat flux
T_w	temperature at $x=0$	τ_t	delay time in establishing temperature gradient
z_q	dimensionless form of τ_q, $\tau_q/(l^2/\alpha)$		
z_t	dimensionless form of τ_t, $\tau_t/(l^2/\alpha)$		

$$\rho c\frac{\partial T}{\partial t} = -\nabla\cdot\vec{q}, \tag{2}$$

where ρ is the density and c is the specific heat. Substituting Eq. (1) into Eq. (2) and eliminating $\vec{q}$ gives

$$\frac{\partial T}{\partial t}+\tau_q\frac{\partial^2 T}{\partial t^2} = \alpha\nabla^2 T+\alpha\tau_t\frac{\partial}{\partial t}\nabla^2 T, \tag{3}$$

where $\alpha = k/(\rho c)$. By setting $\tau_t = 0.0$, Eq. (3) reduces to the classical thermal wave propagation problem (single-phase lag (SPL) model), which has been studied intensively. Therefore Eq. (3) can describe more general cases than the wave equation.

The mathematical form of Eq. (3) is very complex. It includes not only derivatives with respect to space and time, respectively, but also the cross derivative with respect to space–time as well as their higher-order derivatives. In this work, a new numerical method is developed to solve Eq. (3). The new method combines the dual reciprocity boundary element method (DRBEM) with Laplace transforms. It includes three steps. The first step is to transform the governing equation and corresponding initial and boundary conditions into Laplace space by Laplace transform. In this process the time terms can be removed from the original equation. Secondly, the transformed equations are solved in Laplace space by DRBEM. Finally, the solution is transformed back into physical space. A detailed description of the new method is given below. Examples are also presented to demonstrate the validity of the new method, and to illiterate the characteristics of the non-Fourier heat conduction.

2. Procedure of the new numerical method

Eq. (3) can be non-dimensionlized by using:

$$z_q = \frac{\tau_q}{l^2/\alpha},\quad z_t = \frac{\tau_t}{l^2/\alpha},\quad \beta = \frac{t}{l^2/\alpha},\quad \xi = \frac{x}{l},\quad \eta = \frac{y}{l},$$
$$\theta = \frac{T-T_0}{T_w-T_0},$$

where l, T_w and T_0 are the length in the x-direction, the heated (set at $x=0$) and initial temperatures, respectively. The dimensionless form of Eq. (3) can then be rewritten as:

$$\frac{\partial\theta}{\partial\beta}+z_q\frac{\partial^2\theta}{\partial\beta^2} = \nabla^2\theta+z_t\frac{\partial}{\partial\beta}\nabla^2\theta. \tag{4}$$

Taking the following Laplace transform:

$$\bar{\theta}(\xi,\eta,\lambda) = \int_0^\infty \theta(\xi,\eta,\beta)\,\mathrm{e}^{-\lambda\beta}\,\mathrm{d}\beta. \tag{5}$$

Then Eq. (4) is given as follows:

$$\nabla^2\bar{\theta}(\xi,\lambda) = V\bar{\theta}(\xi,\lambda)-C_0, \tag{6}$$

where

$$C_0 = \left[\theta(\xi,0)+z_q\lambda\theta(\xi,0)+z_q\frac{\partial\theta(\xi,0)}{\partial\beta}-z_t\nabla^2\theta(\xi,0)\right]\Big/(1+\lambda z_t)$$

and

$$V = \frac{\lambda(1+\lambda z_q)}{1+\lambda z_t} \tag{7}$$

or

$$\nabla^2\bar{\theta}(\xi,\beta) = b \quad \text{with } b = V\bar{\theta}-C_0. \tag{8}$$

The initial and boundary conditions in physical space should also be transformed into the corresponding ones in Laplace space.

Using the theory of dual reciprocity [10], Eq. (8) will be transformed into the following pure boundary integral equation:

$$c_i\bar{\theta}_i + \int_\Gamma \bar{q}^*\bar{\theta}\,\mathrm{d}\Gamma - \int_\Gamma \bar{\theta}^*\bar{q}\,\mathrm{d}\Gamma = \sum_{j=1}^{N+L}\alpha_j\left(c_i\hat{\bar{\theta}}_{ij} + \int_\Gamma \bar{q}^*\hat{\bar{\theta}}_j\,\mathrm{d}\Gamma - \int_\Gamma \bar{\theta}^*\hat{\bar{q}}_j\,\mathrm{d}\Gamma\right). \quad (9)$$

The terms $\bar{q}^*$, $\hat{\bar{q}}_j$ and $\bar{q}$ in Eq. (9) are defined as $\bar{q}^* = \partial\bar{\theta}^*/\partial n$, $\hat{\bar{q}}_j = \partial\hat{\bar{\theta}}_j/\partial n$ and $\bar{q} = \partial\bar{\theta}/\partial n$, respectively, where n is the unit outward normal to the boundary Γ, and

$$\bar{\theta}^* = \frac{1}{2\pi}\ln\left(\frac{1}{r}\right), \quad \hat{\bar{\theta}}_j = \frac{r^2}{4} + \frac{r^3}{9}.$$

The coefficient c_i can be shown to be $c_i = \gamma/2\pi$ (γ is the internal angle at point i). $\alpha = F^{-1}b$, where each column of F consists of $f_j = 1 + r_j$, and r is the distance between two points. N and L are the numbers of boundary nodes and internal nodes, respectively.

After solving Eq. (8) by DRBEM, the result $\bar{\theta}(\xi,\lambda)$ must be inversely transformed into physical space using Laplace inverse-transform methods [11,12]:

$$\theta_i(\beta) = \frac{\ln 2}{\beta}\sum_{j=1}^{M} w_j\bar{\theta}_{ij} \quad (10)$$

with

$$w_j = (-1)^{(M/2)+j} \times \sum_{k=[(j+1)/2]}^{\min(j,M/2)} \frac{k^{M/2}(2k)!}{((M/2)-k)!k!(k-1)!(j-k)!(2k-j)!}, \quad (11)$$

where the Laplace transform parameter $\lambda_j = j(\ln 2/\beta)$, $i = 1,2,\ldots,N$ is the number of boundary or internal grids, and $j = 1,2,\ldots,M$ is the number of items in convergent series.

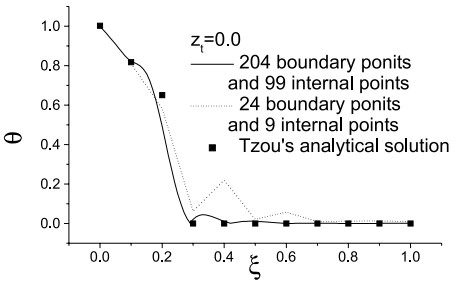

Fig. 1. The effect of the grid distribution for one-dimensional problem when $z_q = 0.05$.

3. Validation of the new method

To demonstrate the validity of the newly developed method, the new method is employed to solve the following one-dimensional problem that has an analytical solution. The problem considered is a non-Fourier heat conduction problem in a one-dimensional spindly slab ($-0.01 \leqslant \eta \leqslant 0.01$ and $0.0 \leqslant \xi \leqslant 1.0$) under the following initial and boundary conditions with the top and bottom walls kept adiabatic:

$$\theta(\xi,\beta) = 1 \quad (\text{at } \xi = 0, \beta > 0), \quad (12)$$

$$\partial\theta(\xi,\beta)/\partial\xi = 0 \quad (\text{at } \xi = 1, \beta > 0), \quad (13)$$

$$\theta(\xi,\beta) = 0, \quad \partial\theta(\xi,\beta)/\partial\xi = 0 \quad (\text{at } \beta = 0). \quad (14)$$

First, the effect of the grid distribution is investigated. Fig. 1 compares the two grid systems. One can see that a denser grid distribution gives a more accurate solution as expected. Good agreement between the numerical solution and the analytical solutions of Tzou [7] and Antaki [8] for thermal diffusion and thermal wave problems are showed in Figs. 2(a) and (b), respectively.

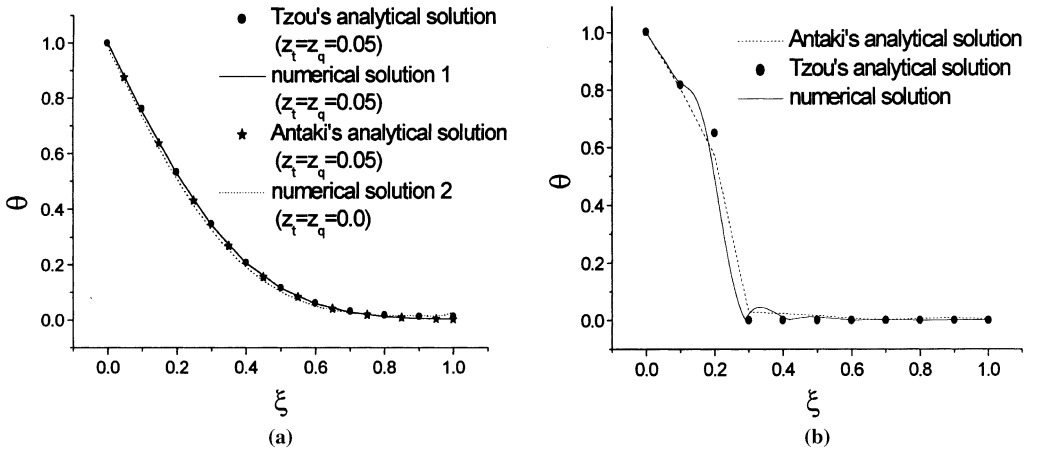

Fig. 2. Comparison between numerical and analytical results: (a) thermal diffusion ($z_q = \beta = 0.05, z_t = 0.05$); (b) thermal wave ($z_q = \beta = 0.05, z_t = 0.0$).

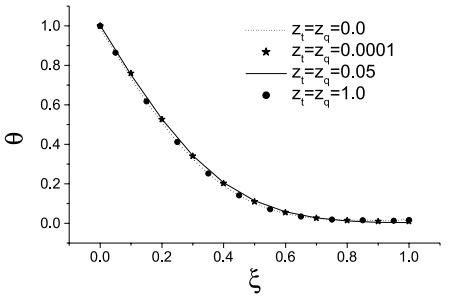

Fig. 3. Influence of different value of $z_t = z_q$ under the initial field of zero-temperature and zero-temperature gradient.

The results show that this numerical method is credible. The numerical result for the classical Fourier heat-conduction equation ($z_t = z_q = 0$) is also drawn in Fig. 2(a). As shown in Fig. 2(a), this result is accordant with the numerical result of DPL model for $z_t = z_q = 0.05$. Different numerical solutions for $z_t = z_q$ under the initial conditions of zero-temperature and zero-temperature gradient are made, and the results are drawn in Fig. 3.

As shown in Fig. 3, no matter what the value of $z_t = z_q \neq 0$ is, the results can all approach to the classical diffusion solution. Then in the following consideration, we will take the $z_t = z_q = 0.05$ as thermal diffusion under the same initial conditions.

4. Non-Fourier heat conduction for isothermal inlet

Next, consider again the one-dimensional heat conduction problem with the initial and boundary conditions defined by Eqs. (12)–(14). This time, fix the value of $z_q = 0.05$, but varying the value of z_t. When $z_t = 0.0$ (i.e., $\tau_t = 0$), the governing equation reduces to the thermal wave equation, while $z_t \neq 0$ corresponds to the case of DPL model, with $z_q = z_t$ as a special case of pure thermal diffusion as considered above. Typical numerical results are drawn in Fig. 4. When $z_t > z_q$ (i.e., $\tau_t > \tau_q$), which some have described as over-diffusion heat conduction [9], it shows such a phenomenon that the lag of heat flux in the region will be smaller than the lag of temperature gradient. From Fig. 4, it can be seen that the temperature distribution curve of over-diffusion heat conduction will become smoother. However, when $z_t \neq 0$, the sharp descent of temperature distribution on space (i.e., the thermal wave front) will not exist. The greater z_t is, the more even the temperature distribution will be. Similar results can be seen in the literature [7,8].

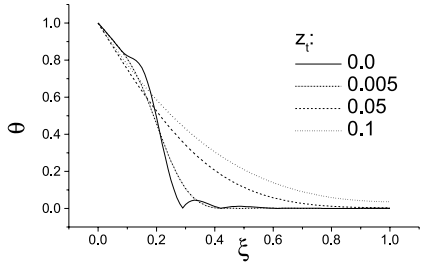

Fig. 4. Dimensionless temperature distribution for different z_t under the condition of isothermal inlet ($z_q = 0.05, \beta = 0.05$).

5. Non-Fourier heat conduction under the pulsed temperature inlet condition

A pulsed temperature on the left boundary causes different heat-conduction rules between the thermal wave and non-Fourier cases. Considering the two-dimensional problem with the geometry showed in Fig. 5, the computation domain is $0.0 \leqslant \xi \leqslant 1.0$ and $0.0 \leqslant \eta \leqslant 0.5$, and there are 50 boundary points and 76 internal points ($\Delta\xi = 0.05, \Delta\eta = 0.10$). The initial conditions are zero-temperature and zero-temperature gradient. A temperature pulse set on the left boundary has non-zero time width.

The boundary conditions are given as:

when $\beta \in [\beta_1, \beta_2]$

$$\begin{cases} \theta(\xi, \eta, \beta) = 1.0 \quad (\text{at } \xi = 0.0 \text{ and } \eta \in [\eta_1, \eta_2]), \\ \dfrac{\partial\theta(\xi, \eta, \beta)}{\partial\xi} = \dfrac{\partial\theta(\xi, \eta, \beta)}{\partial\eta} = 0.0 \quad (\text{others}), \end{cases} \tag{15}$$

when $\beta \notin [\beta_1, \beta_2]$

$$\begin{cases} \theta(\xi, \eta, \beta) = 0.0 \quad (\text{at } \xi = 0.0 \text{ and } \eta \in [\eta_1, \eta_2]), \\ \dfrac{\partial\theta(\xi, \eta, \beta)}{\partial\xi} = \dfrac{\partial\theta(\xi, \eta, \beta)}{\partial\eta} = 0.0 \quad (\text{others}). \end{cases} \tag{16}$$

Here choosing $\beta_1 = 0.05$, $\beta_2 = 0.10$, $\eta_1 = 0.2$ and $\eta_2 = 0.3$, then the three-dimensional dimensionless temperature maps of the single-phase (thermal wave) and dual-phase lag (non-Fourier) heat-conduction problems are drawn in Fig. 6.

Comparing Fig. 6(a) with Fig. 6(b), within the pulse heated time interval (Figs. 6(a1)–(a3) and (b1)–(b3)), the temperature propagation images of the SPL model and the DPL model are almost the same. However, with time

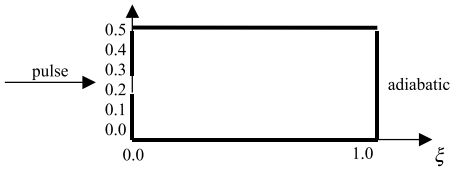

Fig. 5. Geometry condition for two-dimensional problem set pulse.

marching, their differences gradually appear because of the effect of wave reflection and superposition in thermal wave heat conduction. Similar to the one-dimensional results, the temperature near the heated boundary is higher than the pulsed temperature since the non-Fourier heat conduction lags behind the Fourier diffusion. As shown in Fig. 6, during time interval $0.07 < \beta < 0.10$, temperature near the heated wall is higher than the initial

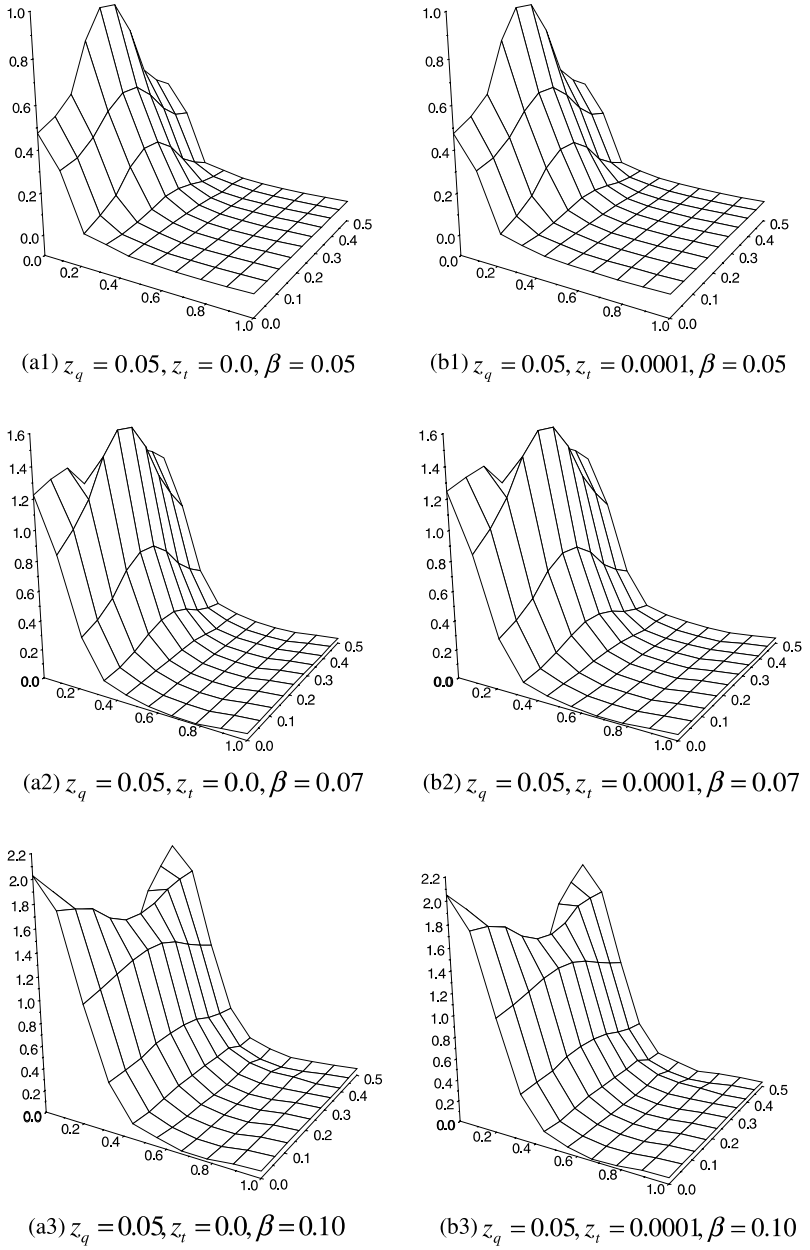

Fig. 6. Three-dimensional figures for the two-dimensional problem with non-zero time width pulse set on the left boundary: (a) thermal wave heat conduction (SPL model); (a1) $z_q = 0.05, z_t = 0.0, \beta = 0.05$, (a2) $z_q = 0.05, z_t = 0.0, \beta = 0.07$, (a3) $z_q = 0.05, z_t = 0.0, \beta = 0.10$, (a4) $z_q = 0.05, z_t = 0.0, \beta = 0.20$, (a5) $z_q = 0.05, z_t = 0.0, \beta = 0.34$, (a6) $z_q = 0.05, z_t = 0.0, \beta = 0.54$; (b) non-Fourier heat conduction (DPL model); (b1) $z_q = 0.05, z_t = 0.0001, \beta = 0.05$, (b2) $z_q = 0.05, z_t = 0.0001, \beta = 0.07$, (b3) $z_q = 0.05$, $z_t = 0.0001, \beta = 0.10$, (b4) $z_q = 0.05, z_t = 0.0001, \beta = 0.20$, (b5) $z_q = 0.05, z_t = 0.0001, \beta = 0.34$, (b6) $z_q = 0.05, z_t = 0.0001, \beta = 0.54$.

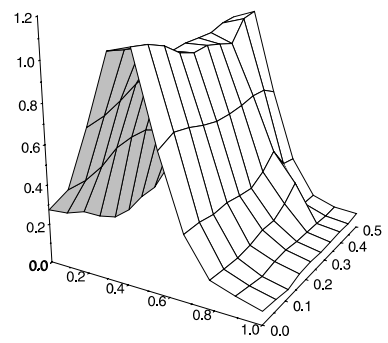

(a4) $z_q = 0.05, z_t = 0.0, \beta = 0.20$

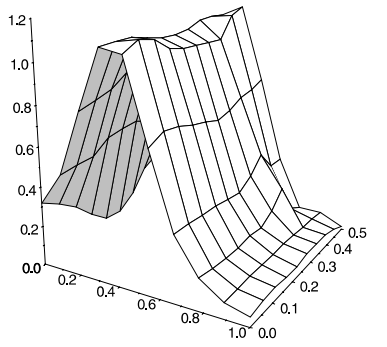

(b4) $z_q = 0.05, z_t = 0.0001, \beta = 0.20$

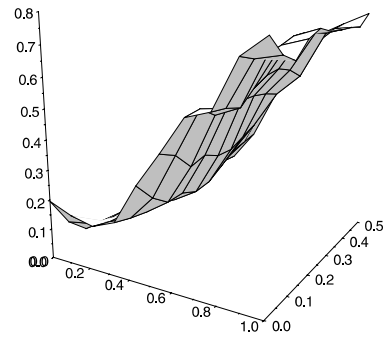

(a5) $z_q = 0.05, z_t = 0.0, \beta = 0.34$

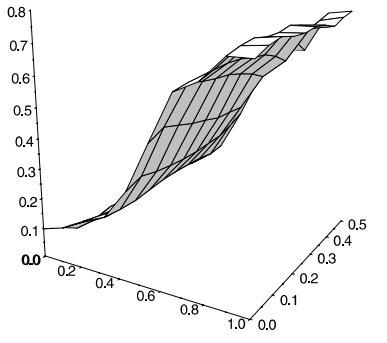

(b5) $z_q = 0.05, z_t = 0.0001, \beta = 0.34$

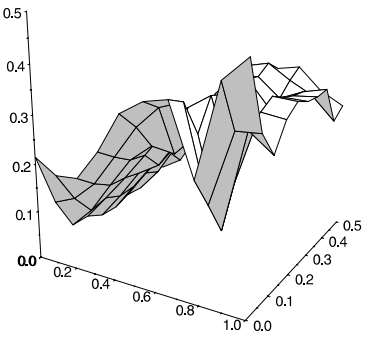

(a6) $z_q = 0.05, z_t = 0.0, \beta = 0.54$

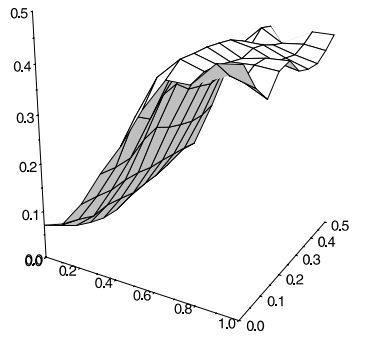

(b6) $z_q = 0.05, z_t = 0.0001, \beta = 0.54$

Fig. 6 (*continued*)

temperature ($\theta = 1.0$). And at the same time, such phenomenon only exists in the narrow space region near the heated wall. Therefore, the delay effect only exists within a short time interval and narrow space domain. Notice that this space–time micro-scale effect has obvious two-dimensional characters. The reflecting and superposing on sideward walls and propagating forwards phenomena of thermal wave can be observed from those Fig. 6(a). For thermal wave heat conduction, the wave effect controls the whole process, and this process shows strongly fluctuant character. While in the case of the DPL model, the total heat-conduction process is jointly controlled by the wave and diffusing effect. With increasing τ_t, the wave effect of heat-conduction process is weakened, and the diffusion gradually increases at the same time.

6. Conclusions

A numerical method combining the dual reciprocity boundary element method with Laplace transforms is used to solve the non-Fourier heat-conduction problem

under different inlet conditions. The differences between the thermal wave heat transfer, the non-Fourier heat conduction and the thermal diffusion heat conduction are numerically computed. Then the following conclusions can be obtained:

1. The numerical method combining the dual reciprocity boundary element method (DRBEM) with Laplace transforms is effective for solving such mathematical equations as the DPL model including derivatives with respect of time, space and space–time cross as well as its higher-order cross derivative. Agreement between the results of the numerical solution and the analytical solutions shows that this method and its results are credible. Furthermore, this paper reports the two-dimensional numerical results of the non-Fourier heat-conduction problem under different boundary conditions.
2. When $z_q = z_t = 0.0$, DPL model degenerates into the classical diffusion model. When $z_q = z_t \neq 0.0$ with zero-temperature and zero-temperature gradient initially, the pure diffusion solution of the DPL model can be also obtained.
3. When $z_q > 0$ is fixed, increasing z_t from zero makes that the heat conduction law is developed from the thermal wave heat conduction into the non-Fourier heat conduction, then into the thermal diffusion heat conduction, and finally into over-diffusion heat conduction.
4. Under the pulsed inlet condition, the space–time micro-scale effect of non-Fourier heat conduction is numerically predicted. This effect has obvious two-dimensional characteristics.

Acknowledgements

The project was supported by the National Natural Scientific Foundation of China (grant No. 59976043) and the National Great Basic Research Development Project of China (grant No. G200026300).

References

[1] M.N. Ozisik, D.Y. Tzou, On the wave theory in heat conduction, J. Heat Transfer 116 (1994) 526–535.
[2] S.D. Brorson, J.G. Fujimoto, E.P. Ippen, Femtosecond electron heat-transport dynamics in thin gold film, Phys. Rev. Lett. 59 (1987) 1962–1965.
[3] C.C. Ackerman, R.A. Guyer, Temperature pulses in dielectric solids, Ann. Phys. 50 (1968) 128–185.
[4] W.Q. Lu, L. Han, Q.M. Fan, W. Guo, The dual-phase lag model of non-Fourier heat conduction in a kind of two-phase mediums, in: B.-X. Wang (Ed.), Heat Transfer Science and Technology 2000, High Education Press, Beijing, 2000, pp. 163–168.
[5] S.I. Anisimov, B.L. Kapeliovich, T.L. Perel's man, Electron emission from metal surfaces exposed to ultra short laser pulses, Sov. Phys. JETP 39 (1974) 375–377.
[6] T.Q. Qiu, C.L. Tien, Heat transfer mechanisms during sort-pulse laser heating of metals, J. Heat Transfer 115 (1993) 834–841.
[7] D.Y. Tzou, A unified field approach for heat conduction from macro- to micro-scales, ASME J. Heat Transfer 117 (1995) 8–16.
[8] P.J. Antaki, Solution for non-Fourier dual phase lag heat conduction in a semi-infinite slab with surface heat flux, Int. J. Heat Mass Transfer 41 (1998) 2253–2258.
[9] D.W. Tang, N. Araki, Wavy, wavelike, diffusive thermal responses of finite rigid slabs to high-speed heating of laser-pulses, Int. J. Heat Mass Transfer 42 (1999) 855–860.
[10] P.W. Partridge, C.A. Brebbia, L.C. Wrobel, The Dual Reciprocity Boundary Element Method, Elsevier Applied Science, London, 1992.
[11] D. Crann, A.J. Davies, J. Mushtaq, Parallel Laplace transform boundary element methods for diffusion problems, in: C.A. Brebbia (Ed.), Boundary Elements XX, Computational Mechanics Publications, Southampton, 1998, pp. 259–267.
[12] H. Stehfest, Numerical inversion of Laplace transforms, Commun. ACM 13 (1970) 47–50.